Inorganic Chemistry

pubs.acs.org/IC Article

Evaluation of Octaethyl-7,17-dioxobacteriochlorin as a Ligand for Transition Metals

David Schnable,§ Nivedita Chaudhri,§ Ruoshi Li, Matthias Zeller, and Christian Brückner*



Cite This: Inorg. Chem. 2020, 59, 2870–2880



ACCESS

Metrics & More



S Supporting Information

ABSTRACT: The propensity of octaethyl-7,17-dioxobacteriochlorin toward the formation of transition metal complexes was evaluated. A variety of M^{II} ions (M = Co, Ni, Cu, Zn, Pd, Ag, and Cd) and Fe(III) could be inserted using standard methodologies or, more often, using more forcing conditions. The stable products were spectroscopically characterized. The solid-state structures of the Ni(II), Cu(II), Pd(II), and Ag(II) complexes could also be determined by single crystal X-ray diffractometry, whereby the [7,17-dioxobacteriochlorinato] chromophore was found to be largely planar in all cases. The rate of Zn(II) insertion into octaethyl-

7,17-dioxobacteriochlorin was less than half that into the corresponding 7-oxochlorin, which itself was about half the rate into the parent octaethylporphyrin. These rate differences reflect the relative decreased basicity of the β -oxo-substituted chromophores and possibly also their decreased conformational flexibility. We compare the basicity of the dioxobacteriochlorin to that of a range of related products of varying reduction state (porphyrin, chlorin, bacteriochlorin), an isomer, and the absence or presence of oxofunctionality, like oxochlorin, chlorin, oxobacteriochlorins, and bacteriochlorin, quantifying the effects of these macrocycle modifications. The work rationalizes earlier reports of the inability of tolyporphin A, a natural product possessing a 7,17-dioxobacteriochlorin chromophore, to form metal complexes and provide a more quantitative understanding of the degree of modulation that β -oxo groups have on the coordination properties of porphyrinoids.

■ INTRODUCTION

Tolyporphins are a family of tetrapyrroles isolated from the cyanobacterium *Tolypothrix nodosa*. They share a unique 7,17-dioxobacteriochlorin chromophore carrying also *C*-glycoside moieties at their β -positions. The most prevalent and well-studied member of this class is tolyporphin A (1).

Tolyporphin A effectively reverses multidrug resistance (MDR) of cancer cells. MDR describes the phenomenon that cells can become resistant to many chemotherapeutics by an overexpression of a transmembrane P-glycoprotein pump

that detoxifies cells by exporting hundreds of chemically unrelated toxins out of cells, thereby lowering their intracellular concentrations. Finding drugs that reverse this significant limitation of cancer chemotherapies is important.

The tolyporphins, however, also exhibit significant cytotoxicity, limiting their therapeutic potential as MDR reversal drugs. Furthermore, it is also known that tolyporphins are effective photosensitizers; like many tetrapyrrolic pigments, upon irradiation with visible light and in the presence of triplet oxygen (3O_2) they produce toxic singlet oxygen (1O_2). Therefore, to more conveniently utilize tolyporphins as potential pharmaceuticals to reverse MDR, at least their phototoxicity must be reduced. Prinsep et al. hypothesized that the insertion of a metal ion into the dioxobacteriochlorin core may reduce its (photo)cytotoxicity; 11 after all, certain metal ions switch off the ability of a photosensitizer to generate singlet oxygen. The authors thus reported the preparation of the Ag(II) and Cu(II) complexes of tolyporphins. These complexes showed considerably lower cytotoxicity. Alas, they were also less potent in reversing MDR.

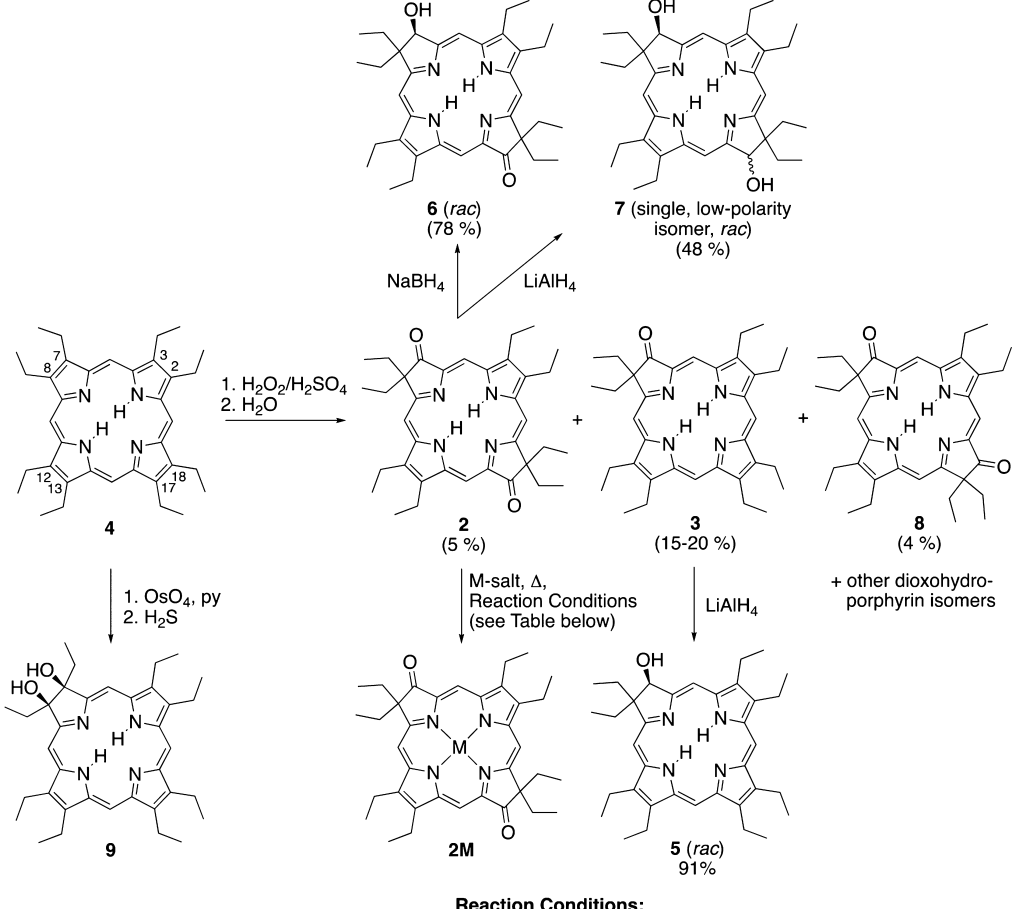
In general, tetrapyrrolic macrocycles are excellent metal chelators for a wide range of metal ions. 12 Thus, it was

Received: November 4, 2019
Published: February 7, 2020



Inorganic Chemistry Article pubs.acs.org/IC

Scheme 1. Synthetic Pathway^a



Reaction Conditions:

5 equiv. M source, solvent, temperature, time, base, isolated yield 2Fe: M = Fe(III)CI FeCl₃·6H₂O, acetic acid reflux, 40 min, -, 70% 2Co: M = Co(II) Co(NO₃)·6H₂O, DMF reflux, 210 min, 10 eq Li₂CO₃, 91% 2Ni: M = Ni(II) Ni(OAc)₂·4H₂O, PhCN reflux, 300 min, -, 84% Cu(OAc)2, DMF reflux, 30 min, -, 83% 2Cu: M = Cu(II) 2Zn: M = Zn(II) ZnCl₂·2H₂O, DMF or pyridine reflux, 210 min, 10 eq Li₂CO₃, 96% PdCl₂, PhCN reflux, 120 min, -, 71% 2Pd: M = Pd(II) 2Ag: M = Ag(II) Ag(OAc), pyridine reflux, 60 min, -, 52% 2Cd: M = Cd(II) CdCl₂·½ H₂O, DMF reflux, 300 min, 10 eq Li₂CO₃, 91%

^aSynthesis of octaethyl-7,17-dioxobacteriochlorin 2, together with 7-oxochlorin 3 and 7,18-dioxobacteriochlorin 8 from octaethylporphyrin 4,⁴⁶ formation of the metal complexes 2M, reduction of 7-oxochlorin 3²⁸ and dioxobacteriochlorin 2, and dihydroxylation of octaethylporphyrin 4. 51,57 Numbering system used shown in compound 4.

surprising that Prinsep et al. reported that, besides the Cu(II) and Ag(II) complexes of 1, no other metal complexes could be prepared. Using stoichiometric excess of the metal salts MgCl₂· 6H₂O, VO(SO₄), FeCl₂·4H₂O (in air), CoCl₂·6H₂O (in air), Ni(NO₃)₃·6H₂O₄ ZnSO₄·7H₂O (the Zn(II) complex was observed under the conditions of ESI+ MS), Na₂[PdCl₄] or Pd(NO₃)₂, Cd(ClO₄)₂, and Pb(NO₃)₂, all in MeOH containing NEt₃ at reflux temperature (65-70 °C) over 20-40 min did not form the expected complexes. 11 Regular porphyrins, however, would have been expected to have inserted at least some of the metal ions. 12 The inability to form the metal complexes might have its origins in an intrinsic inhibition of the 7,17-dioxobacteriochlorin framework toward metal insertion, requiring the use of more forcing conditions. Even if this was not stated, we suspect the thermal instability of tolyporphin A made this approach impossible.

The assumption that the 7,17-dioxobacteriochlorin is deactivated toward the chelation of metal ions is likely because of two effects. First, bacteriochlorins are much less basic than the corresponding chlorins or porphyrins. 13 Compared to the broadly investigated coordination properties of porphyrins, ¹² those of the bacteriochlorins have been studied to a much lesser degree. 14-16 Second, the basicity of the two imine nitrogens in the framework is expected to be further reduced by the presence of the β -oxo-functionalities.

A wide range of β -oxo-porphyrins or β -oxo-hydroporphyrins (excluding here β,β' -dioxo-porphyrins and their secochlorin analogues) has become available, either through manipulations of porphyrins or total syntheses.^{8,20-23} The strong electronic influences of the β -oxo-auxochrome were described (in oxoporphyrins as well as porpholactones). 23-27 The zinc(II), zinc(III), zinc

palladium(II),²⁹ and platinum(II)²⁹ complexes of 7-oxochlorin (3) were reported. 7,12-Dioxoisobacteriochlorin iron(III) complexes are found as prosthetic groups in nature³² and were utilized in the study of the metal complexes of 7,12dioxoisobacteriochlorin model systems aimed at the understanding of the role of the oxo-substituted chromophore. 33-41 Comparably less is known about the coordination properties of the isomeric 7,17-dioxobacteriochlorin system. Nonetheless, in addition to the tolyporphin A copper(II) and silver(II) complexes¹¹ the nickel(II), ²⁴ copper(II), ⁴², ⁴³ palladium(II), ⁴⁴ and platinum(II)⁴⁴ complexes of octaethyl-7,17-dioxobacteriochlorin 2 were formed and characterized. No explicit reference to an assessment of any difficulties to insert the metal ions was made in any of the reports. The group of Lindsey evaluated the conditions for the insertion of metals into a wider range of bacteriochlorins, including β -oxo-derivatives. ¹⁶ Other 7,17dioxobacteriochlorin complexes were formed as a consequence of the synthetic strategy chosen to assemble the macrocycle. 45

We thus set out to characterize the chelation properties of the 7,17-dioxo-8,18-bis-gem-dialkylbacteriochlorin chromophore of the tolyporphins in a more systematic fashion. For this purpose, we chose the model compound octaethyl-7,17dioxobacteriochlorin 2 for its accessibility and predicted thermal stability. 46 We assessed in a qualitative fashion its coordination ability by comparison of the conditions needed to form a range of complexes with other porphyrinic macrocycles. We compared its rate of insertion in comparison to that of the corresponding 7-oxochlorin and porphyrin. We also determined the basicity of the dioxobacteriochlorin chromophore to that of a range of related chromophores of varying reduction state (porphyrin, chlorin, bacteriochlorin) and in the absence or presence of oxo-functionalities. We will present evidence that suggest that the 7,17-dioxobacteriochlorin macrocycle is competent in forming a range of metal complexes but that they require significantly harsher conditions for their formation than the corresponding complexes of the mono-oxochlorin, bacteriochlorin, chlorin, or parent porphyrin. This can be largely attributed to the much-reduced basicity of the 7,17dioxobacteriochlorin chromophore.

■ RESULTS AND DISCUSSION

Preparation of 7-Oxochlorin and 7,17- and 7,18-Dioxobacteriochlorins. Octaethyl-7,17-dioxobacteriochlorin 2 and octaethyl-7-oxochlorin 3, together with all other isomers of the β -diketone series (such as 7,18-dioxobacteriochlorin 8), were prepared by H_2O_2/H_2SO_4 oxidation of multigram quantities of octaethylporphyrin 4, as described by Inhoffen and Nolte (Scheme 1). The reaction itself can be traced back to the work of the groups of Fischer and Johnson. Alternate syntheses are available. 49–52

Reduction Products of Dioxobacteriochlorin 2 and Oxochlorin 3. To isolate the electronic effect of the β -oxo group(s) from the effects of the degree of macrocycle reduction (porphyrin, chlorin, bacteriochlorin), we prepared three derivatives by hydride reduction of the carbonyl groups in β -oxohydroporphyrins **2** and **3** (Scheme 1): known β -hydroxyoctaethylchlorin **5**, ^{28,51,53,54} and novel monoreduced products β -hydroxyoxobacteriochlorin **6** and bis-reduced β -dihydroxybacteriochlorin **7**, respectively. Only the low polarity isomer of the two possible stereoisomers of **7** was utilized. The spectroscopic properties of the alcohols **6** and **7** are equivalent to those of related derivatives **5**5,56 and support their connectivity (see SI for details). Hydroxychlorin **5** shows a

typical chlorin UV—vis spectrum, β -hydroxyoxobacteriochlorin 6 possesses a red-shifted chlorin-type spectrum, whereas β -dihydroxybacteriochlorin 7 exhibits a typical bacteriochlorin spectrum (see SI). Lastly, we included another regular chlorin in this investigation, known vic-dihydroxychlorin 9, prepared by OsO₄-mediated dihydroxylation of porphyrin 4. S1,87

Metal Insertions. The insertion of metal ions into porphyrinic compounds is typically accomplished by heating a solution of the porphyrin and a metal salt in a (coordinating) solvent. The reaction may require the presence of an additional base (or basic solvent). Alternative mechanochemical methods have emerged for some metal ions. S8,59 Generally, the rate-limiting steps of the metal insertion are determined by the considerable kinetic barrier of the planar and relatively rigid porphyrin to distort from planarity to present the iminetype nitrogen atoms to the metal ions in solution, the basicity of the ligand nitrogen atoms, and the intrinsic kinetic lability of the metal ion to be inserted. The sum of these factors determines the solvent/reaction temperature needed for the metal insertion reaction to be successful.

The results of the metal insertion reactions to generate the Fe(III), Co(II), Ni(II), Cu(II), Zn(II), Pd(II), Ag(II), and Cd(II) complexes 2M are presented in Scheme 1. The conditions were derived from a screen of a range of organic and mineral bases. The often modest yields are the result of the small-scale reaction and their workup, including crystallizations; only under the harshest conditions was some minor degree of ligand decomposition observed. Remarkably, the reaction conditions to affect efficient metal insertion are in most cases harsher than the standard reaction conditions¹² for the insertion of the respective metal ion into regular porphyrins. For instance, the insertion of zinc into porphyrins under standard conditions (Zn(II) source in CHCl₃/MeOH at ~65 °C; no need for an extraneous base) 12 failed to yield 2Zn. Instead, hot pyridine (115 °C) or DMF (153 °C) in the presence of lithium carbonate was required. Likewise, expedient nickel insertion required PhCN (at 191 °C) instead of hot pyridine or DMF. Others, like the insertion of Ag(II) by disproportionation of an Ag(I) source, take place in the customary solvent pyridine, albeit the yield of the reaction is relatively low after 60 min and we found it necessary to degas the solution to prevent a further reduction of yield by way of decomposition of the ligand. Otherwise we note the thermal stability of the dioxobacteriochlorin ligand, even at extended times at elevated temperatures under oxic conditions. Other metals were tested but failed to form complexes with 2 under all conventional, thermal conditions tested, including V(IV) (as vanadyl, VO²⁺), Cr(II), Sn(II), and Au(III). However, some of those (kinetically inert) metals are also not readily inserted into porphyrins.

UV-vis Spectroscopic Properties of the Metal Complexes. The normalized UV-vis absorption spectra of free base 2 and its metal complexes 2M are shown in Figure 1 (and tabulated in Table S1). Upon insertion of the metal ions into free base 2, the UV-vis absorption spectra of 2M amplify the split of the Soret bands already present in the free base. The prominent single Q-band (and λ_{max} band) of the free base is retained and, depending on the particular metal ion, at essentially the same position (for 2Fe), slightly hypsochromically (for the 4d element complexes 2Cd, 2Ag, and 2Pd), or bathochromically (for the 3d element complexes 2Co, 2Cu, 2Zn, and 2Ni) shifted. The other less prominent Q-bands of the free base become even less so upon metalation.

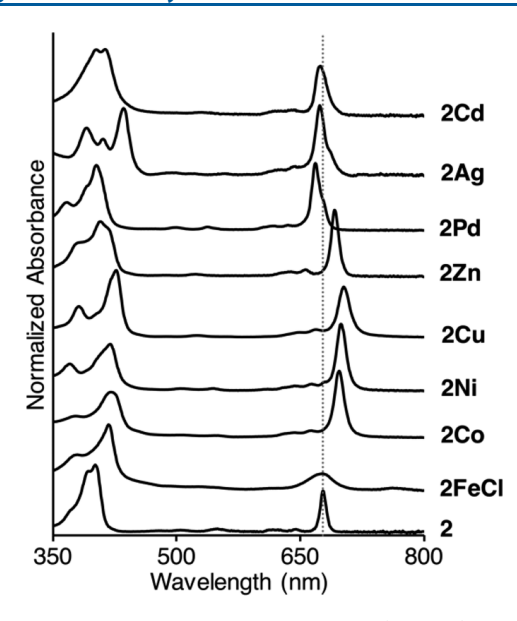


Figure 1. Stacked normalized UV—vis spectra (CH₂Cl₂) of free-base **2** and its metal complexes **2M** indicated. A vertical dotted line at 677 nm (λ_{max} of **2**) serves as a reference line. See Supporting Information for full-scale spectra.

Crystallographic Analysis. XRD-quality single crystals could be grown for the Cu(II), Ni(II), Ag(II), and Pd(II) complexes of octaethyl-7,17-dioxobacteriochlorin 2 (Figure 2; for details, see SI). All of the structures were found to be almost perfectly planar, possessing Δ_{24} RMS value of significantly less than 0.1 Å with the largest deviation observed, as expected, ¹⁹ for the complex with the smallest ion, 2Ni. A survey of crystal structures of 4M deposited at the CCDC reveals that the complexes of 2 tend toward more planar conformations, that is, exhibiting smaller Δ_{24} values when compared to most complexes of 4 with the same metal ion. The Δ_{24} values for some 4Ni complexes are larger (0.46⁶¹ or 0.30⁶²) than that for 2Ni (0.075), though more planar polymorphs are also known (0.03).⁶³ Overall, this may suggest a larger stiffness of the 7,17-dioxobacteriochlorin chromophore and may contribute to the markedly increased difficulty of inserting metals into it. Others have argued on the basis of electrochemical experiments that the oxo-groups increase the flexibility of the macrocycle. ²⁴ For all four complexes, the displacement of the metal from the N_4 plane is found to be less than 0.01 Å. This necessitates increased in-plane "stretching" of the macrocycle to accommodate larger metal ions within the ring. This is observed by the generally increasing diagonal N_1 – N_3 distances as the size of the metal ion increases (e.g., from 4.107(2) to 4.263(4) Å for **2Cu** and **2Ag**, respectively).

Relative Metal Insertion Rates. To provide a more quantitative measure of the generally perceived slower metal ion insertion rates for dioxobacteriochlorin 2, we directly compared its zinc(II) insertion rate with that for oxochlorin 3 (forming 3Zn)^{28,29} and the parent octaethylporphyrin 4 (forming 4Zn)⁶⁴ using identical metal ion insertion conditions (Figure 3). Evidently, the multistep metathesis reactions are

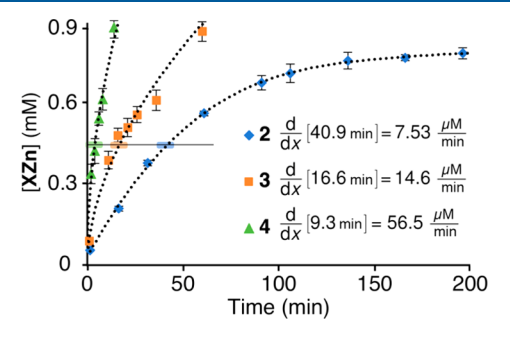


Figure 3. Relative rates of zinc insertion into porphyrin 4, oxochlorin 3, and dioxobacteriochlorin 2 under identical reaction conditions (starting concentrations: $[X] = 8.8 \times 10^{-4} \text{ M}$, $[Zn(OAc)_2] = 4.4 \times 10^{-3} \text{ M}$ (5.00 equiv); combined in 10.0 mL DMF with 15.0 mg Li₂CO₃, 154 °C). The lines of best fit are higher order polynomial functions. The horizontal markers at 0.45 M, the 50% conversion point, indicate the points at which the slope was determined; error bars indicate standard error.

complex as we could not fit the reaction kinetics to simple rate laws. Thus, for the purpose of this comparison the slope of the best-fit function at the point where the product concentration [XZn] reaches the half-conversion point (0.445 mM) was determined. In this manner, the relative rates are measured to be 7.53, 14.6, and 56.5 μ M/min for 2, 3, and 4, respectively. Thus, relative to the rate of the fastest

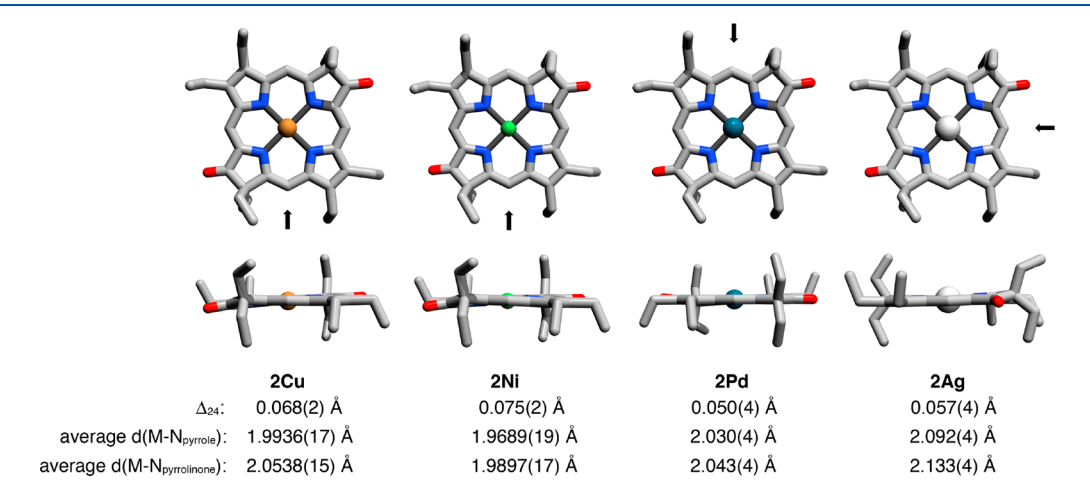


Figure 2. Stick representation of the X-ray single-crystal structures of the metal complexes 2M indicated. The arrow in the top view indicates the direction of the side view below. $\Delta_{24} = RMSD$ of all macrocycle C and N atoms from the mean plane defined by them. For experimental details, see SI.

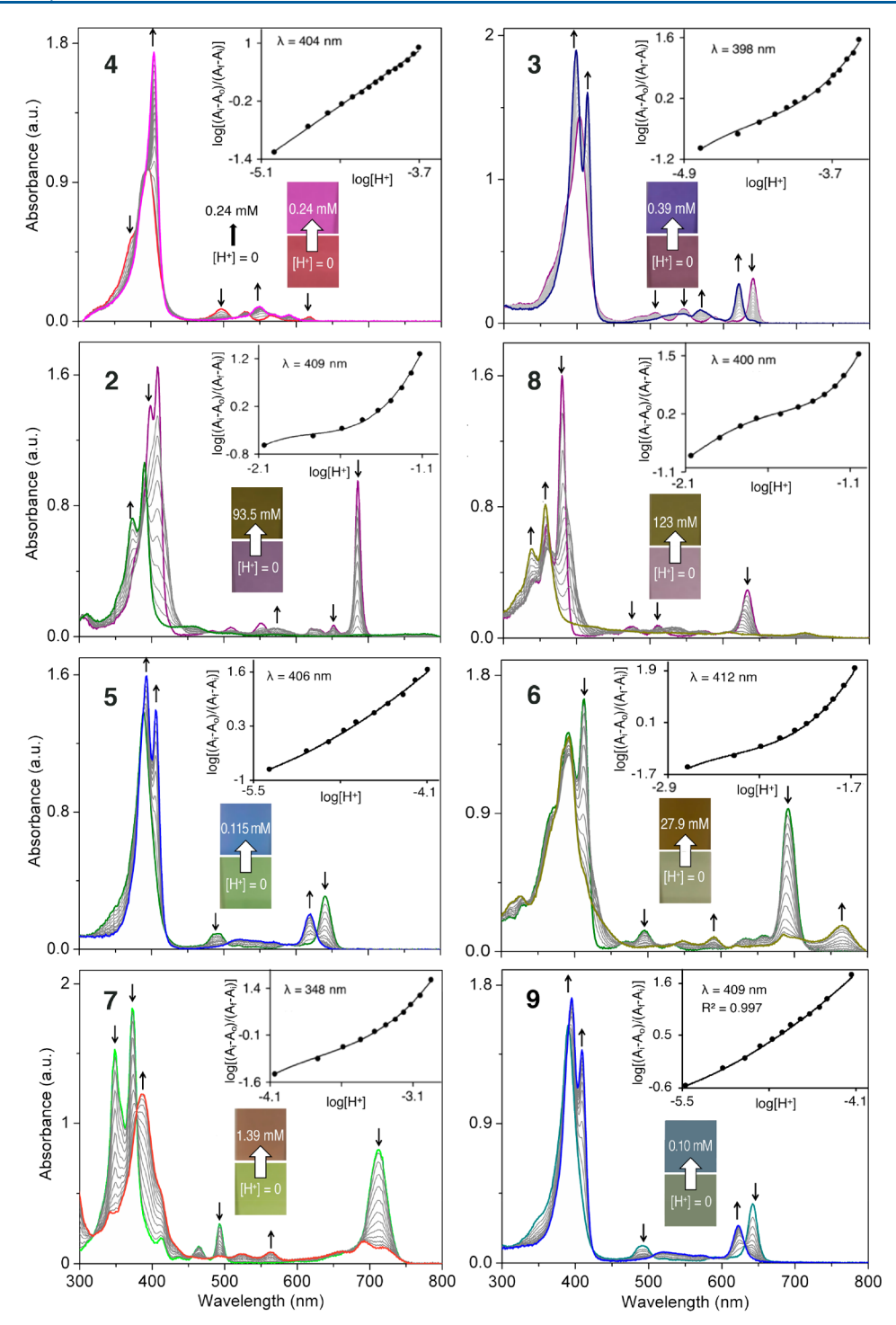


Figure 4. UV—vis titration of octaethylporphyrin 4 (7.18 \times 10⁻⁶ M), 7-oxochlorin 3 (1.82 \times 10⁻⁵ M), 7,17-dioxochlorin 2 (2.12 \times 10⁻⁵ M), its isomer 7,18-dioxochlorin 8 (1.41 \times 10⁻⁵ M), 7-hydroxychlorin 5 (1.52 \times 10⁻⁵ M), 7-hydroxy-17-oxobacteriochlorin 6 (4.23 \times 10⁻⁵ M), 7,17-dihydroxybacteriochlorin 7 (5.88 \times 10⁻⁵ M), and 7,8-dihydroxychlorin 9 (1.83 \times 10⁻⁵ M) (all in CH₂Cl₂) with TFA in the [TFA] range indicated. Insets show a best fit Hill plot. Color fields show the color of the porphyrinoids before and after the addition of TFA. For further details, see SI.

ligand porphyrin 4 (set to 1), oxochlorin 3 is about four times slower and dioxobacteriochlorin 2 is about another factor of 2 slower (for a total of 7.5-fold relative to the rate for 4).

UV—**vis Titrations.** To quantitatively determine the differences in basicity of the oxohydroporphyrins versus porphyrins and the corresponding hydroporphyrins, we performed UV—vis titrations with trifluoroacetic acid (TFA) and base (tetrabutylammonium hydroxide, TBAOH). Next to the three species porphyrin **4**, oxochlorin **3**, and dioxobacterio-

chlorin **2**, we also included hydroxychlorin **5**, hydroxyoxobacteriochlorin **6**, dihydroxybacteriochlorin **7**, and **2**,3-dihydroxychlorin **9**. This allows us to distinguish between the effects of the oxo-functionalities and the intrinsic change of basicity of the various reduction states of the chromophore (plus the alcohol functionality). Lastly, we also included **7**,18-dioxobacteriochlorin **8**, an isomer of the **7**,17-dioxobacteriochlorin **2**, as a test for the influence of the relative positions of the two β -oxo-functionalities.

All compounds showed strong halochromic responses upon addition of TFA (Figure 4). Across the series, the colors of the compounds (free base as well as protonated) and, correspondingly, their general UV—vis spectra, vary widely. Generalized, however, the changes follow the established patterns for many porphyrinoids: Upon protonation, the free base Soret bands give way to new, often hypsochromically shifted bands, and the number of Q-bands is reduced, simplifying the overall appearance of the spectra; the new $\lambda_{\rm max}$ band is frequently red-shifted.

The titration curves of some porphyrinoids (like porphyrin 4 or chlorin 5) show clear isosbestic points and the corresponding Hill plots are linear and show positive cooperativity, indicating one-step protonation (by two protons), as observed for regular porphyrins and chlorins (with the first protonation constant lower than the second).66-68 Select chlorins are also known that can be monoprotonated. 65,69 On the other hand, all β -oxo-functionalized derivatives show no isosbestic points and convoluted Hill plots, indicative of complex protonation behavior involving multiple binding sites; for diketone isomer 2, the complex, multistage protonation behavior was noted previously.⁴⁴ Whether diprotonation is always achieved also remains unclear. 65 Likewise, the IR spectra of oxochlorin 3 and dioxobacteriochlorin 2 in the presence of TFA were inconclusive as to whether oxo-protonation is taking place. Thus, no pK_h values were derived. Nonetheless, we took the absolute [TFA] concentrations at half the end point value of the titration of the porphyrinoids with acid $(^{[TFA]}/_2 \text{ value})$ as a suitable metric to compare their relative basicities.

The $^{[TFA]}/_2$ value ranks the porphyrinoids investigated in the order of decreasing amount of [TFA] needed for half-protonation, that is, increasing order of basicity: dioxobacteriochlorin **2** $(4.27 \times 10^{-2} \text{ M}) <$ dioxobacteriochlorin **8** $(3.42 \times 10^{-2} \text{ M}) <$ hydroxyoxobacteriochlorin **6** $(1.02 \times 10^{-2} \text{ M}) <$ dihydroxybacteriochlorin **7** $(4.27 \times 10^{-4} \text{ M}) <$ oxochlorin **3** $(1.02 \times 10^{-4} \text{ M}) <$ octaethylporphyrin **4** $(6.14 \times 10^{-5} \text{ M}) <$ hydroxychlorin **5** $(2.14 \times 10^{-5} \text{ M}) <$ dihydroxychlorin **9** $(1.36 \times 10^{-5} \text{ M})$ (Figure 5). Thus, increase of the number of β -oxogroups drastically decreases the basicity of the chromophore

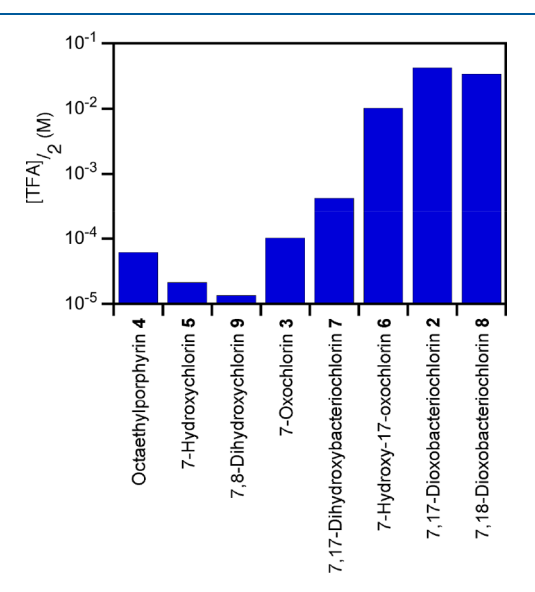


Figure 5. Bar graph of the $[TFA]/_2$ values determined for the compounds indicated (cf. to Figure 4).

over 3 orders of magnitude (comparing basicity of 4 to that of 3 and 2/8). Inversely, stepwise reduction of the β -oxo functionalities in the bacteriochlorin (2 to 6 to 7) and chlorin series (3 to 5) increases the basicity significantly, whereby the removal of one of two oxo-groups has less of an effect than the removal of the second. The basicities of the dioxobacteriochlorin regioisomers 2 and 8 vary slightly from each other, reflecting their electronic differences, a circumstance also observed and rationalized in the *meso*-aryldilactone regioisomers. Bacteriochlorins are, as expected, less basic than the porphyrins and chlorins but we find against expectations the β -hydroxychlorins 5 and 9 to be slightly more basic than the corresponding porphyrin 4. We attribute this to the effects of the electron-rich benzylic alcohol functionalities.

None of the compounds described above showed any major halochromic response upon addition of base (TBAOH in CH_2Cl_2), even at large stoichiometric excess (see SI). At most, minor changes (like in 9) may be attributable to an onset of the deprotonation of an alcohol moiety. Thus, the NH functionalities of the dioxobacteriochlorins neither possess a particularly strong acidity (as corroles, for example, exhibit), or are the β -oxo functionalities accessible to nucleophilic attack under the conditions tested (as the β -oxo functions of some meso-pentafluorophenyl-substituted porpholactones are).

CONCLUSIONS

In conclusion, the metal ions Fe(III), Co(II), Ni(II), Cu(II), Zn(II), Cd(II), Ag(II), and Pd(II) can be inserted into octaethyl-7,17-dioxobacteriochlorin 2 to form the corresponding complexes 2M. The single crystal X-ray structures of 2Cu, 2Ni, 2Pd, and 2Ag prove the complexes to be essentially planar. Arguably, they are slightly more planar than the corresponding oxochlorin or porphyrin complexes, suggestive of a larger conformational rigidity of the dioxobacteriochlorin chromophore. The zinc(II) insertion kinetics for dioxobacteriochlorin isomer 2 is ~4-fold slower than the corresponding reaction for oxochlorin 3, and ~7.5-fold slower compared to the rate observed for octaethylporphyrin 4. The slow kinetics necessitate the use of more forceful reaction conditions than traditionally employed for the metal insertion to be completed within a few hours of reaction time. The basicity of the inner nitrogen atoms, ranked in the order of dioxobacteriochlorins < hydroxyoxobacteriochlorin « dihydroxybacteriochlorin < oxochlorin < porphyrin < hydroxychlorin ~ dihydroxychlorin, spanning a range 3 orders of magnitude, may be primarily responsible for the slow reaction kinetics of the metal insertion reaction, while the inferred increased rigidity of the dioxobacteriochlorin framework may add to this. Our findings rationalize why Prinsep et al. could not form a number of metal complexes of tolyporphin A 1 under the relatively mild conditions tested.

On the other hand, the retardation of the metal insertion rate by the β -oxo-functionalities in, for example, 7,17-dioxobacteriochlorin **2**, are somewhat contradicting findings by Lindsey and co-workers that found that electron-with-drawing substituents helped in the metal insertion into bacteriochlorins, ¹⁶ albeit the effects of β -oxo-functionalities were not tested. This suggests that β -oxo-functionalities may have more profound electronic and conformational effects on the macrocycle than many other substituents, and their large effect on the macrocycle electronic structure supports this.

Multiple examples of β -oxo- and β -dioxohydroporphyrins have become known in recent years and the unique auxochromic effects of the β -oxo-functionality have become to be understood. Some of the free base compounds, or their metal complexes, were described to possess useful optical or electrochemical properties. This study lays the basis for the further investigation of the metal complexes of other β -oxoporphyrinoids for which, by extension, we assume the same retarded metal insertion kinetics to be operational.

EXPERIMENTAL SECTION

Instruments. ¹H NMR and ¹³C NMR spectra were recorded using Bruker AVANCE III 400 and 500 MHz spectrometers from solutions in CDCl₃. UV/vis spectra were obtained using Varian Cary 50 or 100 Bio spectrometers in the solvents indicated. IR spectra were recorded from neat material on a Bruker Alpha FTIR spectrometer using an attenuated total reflection (ATR) diamond crystal. Low- and high-resolution SI spectra were recorded from CH₃CN solutions (~10⁻⁶ M) using AB Sciex API 2000 Triple Quadrupole and AB Sciex QStar Elite Quadrupole-TOF MS instruments, respectively.

Materials. 7-Oxochlorin 3, 7,17-dioxobacteriochlorin 2, and 7,18-dioxobacteriochlorin 8 were prepared by H_2O_2/H_2SO_4 oxidation of octaethylporphyrin 4, as described in the literature. Hown hydroxychlorin 5 was, in a variation to literature procedures, 13,53 prepared by LiAlH₄ reduction of 7-oxochlorin 3 (a procedure and complete data are included for comparison). Chlorin diol 9 was also prepared as described. How of the materials were analytical grade from commercial sources and were used as received. Silica gel 60 aluminum-backed 250 μm analytical TLC plates, silica gel 60 glass-backed 250 μm analytical TLC plates, Brockmann I (50–200 μm) basic alumina, and flash column silica gel (premium grade, 60 Å, 40–75 μm) were provided by Sorbent Technologies, Atlanta, GA.

[Octaethyl-7,17-dioxobacteriochlorinato]zinc(II) (2Zn). Free base dioxobacteriochlorin 2 (11.6 mg, 2.0×10^{-5} mol), ZnCl₂·H₂O $(12.2 \text{ mg}, 8.9 \times 10^{-5} \text{ mol}, 4.5 \text{ equiv})$, and 18 mg Li₂CO₃ were dissolved in DMF (10 mL) and heated to reflux for 3.5 h. The solution was cooled to rt and then slowly diluted with DI water (\sim 75 mL). The precipitate formed was isolated by microfiltration. Recrystallization by solvent exchange from CH₂Cl₂/hexanes provided green microcrystals in 96% yield (12.4 mg, 2.0×10^{-5} mol): MW = 628.3 g/mol; $R_f = 0.10$ (silica- 25% hexanes/CH₂Cl₂). ¹H NMR (500 MHz, CDCl₃, 25 °C): δ 9.54 (s, 1H), 8.88 (s, 1H), 3.87–3.80 (m, 8H), 2.69-2.65 (q, ${}^{3}J$ = 7.4 Hz, 8H), 1.79-1.74 (m, 6H), 0.42 (t, ${}^{3}J$ = 7.4 Hz, 6H). 13 C NMR (125 MHz, CDCl₃, 25 °C): δ 209.5, 158.2, 148.5, 147.1, 143.0, 142.2, 141.4, 95.1, 94.9, 60.2, 31.7, 19.53, 19.34, 18.39, 18.23, 8.4 ppm. UV-vis (CH₂Cl₂) $\lambda_{\rm max}$ (log ε): 382 (4.69), 407 (4.88), 691 (4.97) nm. HR-MS (ESI+, 100% CH₃CN, TOF): m/ z calc'd for $C_{36}H_{44}N_4O_2Zn$, 628.2750 (for M⁺); found, 628.2789.

[Octaethyl-7,17-dioxobacteriochlorinato]copper(II) (2Cu). Free base dioxobacteriochlorin 2 (9.7 mg, 1.71×10^{-5} mol) and Cu(OAc)₂ (16.2 mg, 9.2×10^{-5} mol, 5.4 equiv) were dissolved in DMF (10 mL) and heated to reflux for 30 min. The solution was cooled to room temperature and then diluted with DI water (~75 mL) followed by microfiltration. Recrystallization from CH₂Cl₂/hexanes provided the product as green crystals in 83% yield (8.8 mg, 1.4×10^{-5} mol): MW = 627.3 g/mol; $R_{\rm f}$ = 0.37 (silica-25% hexanes/CH₂Cl₂). UV-vis (CH₂Cl₂) $\lambda_{\rm max}$ (log ε): 385 (4.65), 428 (5.01), 705 (4.87) nm. HR-MS (ESI+, 100% CH₃CN, TOF): m/z calc'd for C₃₆H₄₄N₄O₂Cu, 627.2755 (for M⁺); found, 627.2805.

[Octaethyl-7,17-dioxobacteriochlorinato]nickel(II) (2Ni). Free base dioxobacteriochlorin 2 (10.4 mg, 1.8×10^{-5} mol) and Ni(OAc)₂·4H₂O (22.0 mg, 8.8×10^{-5} mol, 4.8 equiv) were dissolved in benzonitrile (10 mL) and heated to reflux for 5 h. The solution was cooled to rt, diluted with CH₂Cl₂, and twice washed with equal volume of DI water. The organic fraction was isolated and dried over Na₂SO₄, then reduced by rotary evaporation, followed by drying

under a stream of dry N₂ overnight. The crude material was purified by column chromatography (silica-25% hexanes/CH₂Cl₂). Recrystallization by precipitation from DMF/water provided the nickel complex 2Ni in 84% yield (9.6 mg, 1.5 × 10⁻⁵ mol): MW = 622.3 g/mol; $R_{\rm f}=0.45$ (silica-25% hexanes/CH₂Cl₂). UV-vis (CH₂Cl₂) $\lambda_{\rm max}$ (log ε): 370 (3.51), 419 (3.75), 699 (3.92) nm. HR-MS (ESI+, 100% CH₃CN, TOF): m/z calc'd for C₃₆H₄₄N₄O₂Ni, 622.2812 (for M⁺); found, 622.2805.

[Octaethyl-7,17-dioxobacteriochlorinato]cobalt(II) (2Co). Free base dioxobacteriochlorin 2 (10.1 mg, 1.8 × 10^{-5} mol), $Co(NO_3)_2$ · $6H_2O$ (31.2 mg, 1.1 × 10^{-4} mol, 6.0 equiv) and 15.7 mg Li_2CO_3 were combined in DMF (10 mL) and heated to reflux for 3.5 h. The solution was cooled to rt and then slowly diluted with DI water (~75 mL). The precipitate formed was isolated using microfiltration. Recrystallization by solvent exchange from CH_2Cl_2 /hexanes provided 2Co as green crystals in 91% yield (10.1 mg, 1.6 × 10^{-5} mol): MW = 623.3 g/mol; $R_f = 0.38$ (silica-25% hexanes/ CH_2Cl_2). UV-vis (CH_2Cl_2) λ_{max} (log ε): 378 (4.37), 420 (4.70), 697 (4.86) nm. HR-MS (ESI+, 100% CH_3CN , TOF): m/z calc'd for $C_{36}H_{44}N_4O_2Co$, 623.2796 (for M^+); found, 623.2761.

[Octaethyl-7,17-dioxobacteriochlorinato]iron(III) Chloride (2FeCl). 2FeCl was prepared by combining free base dioxobacteriochlorin 2 (9.6 mg, 1.7×10^{-5} mol) and FeCl $_3$ ·6H $_2$ O (29.0 mg, 9.9×10^{-4} mol, 5.8 equiv) in acetic acid (10 mL) and heated to reflux for 40 min. The solution was chilled in an ice bath, poured onto crushed ice (~15 g), mixed with brine (10 mL), and then extracted with CH $_2$ Cl $_2$ (~30 mL). The organic layer was isolated, washed with 0.5 M aq HCl, dried over anhydrous Na $_2$ SO $_4$, then reduced to dryness using rotary evaporation. Recrystallization by solvent exchange from CH $_2$ Cl $_2$ /hexanes provided green crystals of 2FeCl in 70% yield (7.7 mg, 1.2×10^{-5} mol): MW = 655.3 g/mol; R_f = 0.05 (silica-0.5% MeOH/CH $_2$ Cl $_2$). UV-vis (CH $_2$ Cl $_2$) $\lambda_{\rm max}$ (log ε): 377 (3.36), 411 (3.51), 675 (3.16) nm. HR-MS (ESI+, 100% CH $_3$ CN, TOF): m/z calc'd for C $_3$ 6H $_4$ 4N $_4$ O $_2$ Fe, 620.2814 (for M $^+$); found, 620.2834.

[Octaethyl-7,17-dioxobacteriochlorinato]cadmium(II) (2Cd). 2Cd was prepared by combining free base dioxobacteriochlorin 2 (9.8 mg, 1.7×10^{-5} mol), CdCl₂·H₂O (20.3 mg, 8.9×10^{-5} mol, 5.1 equiv), and Li₂CO₃ (15.6 mg) in DMF (10 mL) and heating to reflux for 5 h. The solution was then cooled to rt and then slowly diluted with DI water (~75 mL). The precipitate formed was isolated using microfiltration. Recrystallization by solvent exchange from CH₂Cl₂/hexanes provided 2Cd as green crystals in 91% yield (10.7 mg, 1.6×10^{-5} mol). MW = 676.2 g/mol; $R_{\rm f} = 0.20$ (silica-25% hexanes/CH₂Cl₂). UV-vis (CH₂Cl₂) $\lambda_{\rm max}$ (log ε): 402 (3.50), 413 (3.50), 672 (3.35) nm. HR-MS (ESI+, 100% CH₃CN, TOF): m/z calc'd for C₃₆H₄₄N₄O₂Cd, 678.2498 (for M⁺); found, 678.2538.

[Octaethyl-7,17-dioxobacteriochlorinato]silver(II) (2Ag). Free base dioxobacteriochlorin 2 (10.6 mg, 1.9×10^{-5} mol) and Ag(OAc) (6.4 mg, 3.8×10^{-5} mol, 2.0 equiv) were dissolved in deoxygenated pyridine (8 mL) and heated under N_2 to reflux for 1 h. The solution was then cooled to rt, diluted with CH_2Cl_2 , and washed twice with equal volumes of DI water. The organic fraction was isolated and reduced to dryness by rotary evaporation. The crude material was purified by column chromatography (silica-50% hexanes/CH₂Cl₂). Recrystallization from CH_2Cl_2 /hexanes provided 2Ag in 52% yield (6.5 mg, 9.6×10^{-6} mol): MW = 672.6 g/mol; R_f = 0.50 (silica-25% hexanes/CH₂Cl₂). UV—vis (CH_2Cl_2) λ_{max} (log ε): 391 (4.27), 411 (4.15), 435 (4.42), 673 (4.42) nm. HR-MS (ESI+, 100% CH_3CN , TOF): m/z calc'd for $C_{36}H_{44}N_4O_2Ag$, 671.2515 (for M^+); found, 671.2560.

[Octaethyl-7,17-dioxobacteriochlorinato]palladium(II) (2Pd). 2Pd was prepared from free base 7,17-dioxobacteriochlorin 2 (10.4 mg, 1.8×10^{-5} mol) and PdCl₂·6H₂O (17.4 mg, 1.8×10^{-5} mol, 5.4 equiv) in benzonitrile (10 mL) heated to reflux for 1h. The solution was cooled to rt, diluted with CH₂Cl₂, and washed twice with equal volumes of DI water, then the organic fraction was isolated, dried over Na₂SO₄, and reduced by rotary evaporation, followed by drying under a stream of dry N₂ overnight. The crude material was purified by column chromatography (silica-25% hexanes/CH₂Cl₂). Recrystallization by precipitation from DMF/water provided 2Pd in

71% yield (8.7 mg, 1.3×10^{-5} mol). MW = 670.3 g/mol; $R_{\rm f}$ = 0.67 (silica-CH₂Cl₂). ¹H NMR (500 MHz; CDCl₃): δ 9.65 (s, 2H), 8.94 (s, 2H), 3.87–3.79 (m, 8H), 2.72 (qd, J = 13.4, 7.3 Hz, 8H), 1.80 (dt, J = 15.3, 7.6 Hz, 12H), 0.47 (t, J = 7.4 Hz, 12H). UV–vis (CH₂Cl₂) $\lambda_{\rm max}$ (log ε): 366 (3.79), 402 (4.15), 668 (4.16) nm. HR-MS (ESI+, 100% CH₃CN, TOF): m/z calc'd for C₃₆H₄₄N₄O₂Pd, 670.2499 (for M⁺); found, 670.2517.

Octaethyl-7-hydroxychlorin (5). 7-Oxochlorin 4 (50 mg, 9.07 × 10⁻⁵ mol) was dissolved in dry THF (2 mL). To this, a suspension of $LiAlH_4$ (10 mg, 2.7×10^{-4} mol, 3 equiv) in THF (1.5 mL) was added at 0 °C under N2 and stirred for 5 min. The reaction mixture was quenched by slurrying with Glauber's salt (Na₂SO₄·10H₂O, about 1.5 g) and the resulting mixture was filtered through a pad of Celite, and the pad was washed with CH2Cl2. The combined filtrates were reduced by rotatory evaporation. The crude solid was dissolved in a minimum amount of CH₂Cl₂ and purified by column chromatography (silica, 100% CH₂Cl₂, followed by 2% acetone in CH₂Cl₂) to provide the product in 91% yield (46 mg, 8.32×10^{-5} mol). Data for the known compound are included for comparison. MW = 552.8 g/mol; $R_f = 0.19$ (silica-CH₂Cl₂). ¹H NMR (300 MHz, CDCl₃): δ 9.78 (d, J = 3.3 Hz, 2H), 9.20 (s, 1H), 8.79 (s, 1H), 6.53 (s, 1H), 4.07-3.87 (m, 12H), 2.71 (s, 1H), 2.61-2.51 (m, 3H), 2.35-2.25 (m, 1H), 1.89-1.79 (m, 18H), 0.97 (t, J = 7.2 Hz, 3H), 0.74 (t, J = 7.2 Hz, 3H), 2.55 (s, 2H). UV-vis (CH₂Cl₂) $\lambda_{\rm max}$ (log ε): 390 (5.02), 493 (3.85), 521 (3.25), 588 (3.31), 611 (3.26), 642 (4.38). HR-MS (ESI +, 100% CH₃CN, TOF): m/z calc'd for C₃₆H₄₈N₄O, 553.3901 (for MH+): found, 553,3936.

Octaethyl-7-hydroxy-17-oxobacteriochlorin (6). A solution of octaethyl-7,17-dioxobacteriochlorin 2 (50 mg, 8.82×10^{-5} mol) in THF (3 mL) was stirred under N₂ on an ice bath. NaBH₄ (17 mg, 4.4 \times 10⁻⁵ mol, 5 equiv) was added (at 0 °C) and the reaction mixture was stirred for 24 h at ambient temperature. Then CH₂Cl₂ (20 mL) was added and the mixture was washed with a sat'd ag solution of NH₄Cl. The organic layer was separated, dried over anhydrous Na2SO4, and filtered. The filtrate was reduced to dryness using rotatory evaporation. The residue was purified by silica-gel column chromatography (silica, CH_2Cl_2) to yield 6 in 78% (39 mg, 6.86 \times 10^{-5} mol) yield. MW = 568.8 g/mol; $R_f = 0.33$ (silica-CH₂Cl₂). ¹H NMR (400 MHz; CDCl₃): 9.60 (s, 1H), 9.05 (s, 1H), 8.82 (s, 1H), 8.67 (s, 1H), 6.40 (s, 1H), 3.95–3.84 (m, 8H), 2.64 (q, J = 7.3 Hz, 5H), 2.57-2.44 (m, 3H), 2.26 (dt, J = 14.8, 7.4 Hz, 1H), 1.81-1.73(m, 12H), 1.00 (t, 7.4 Hz, 3H), 0.82 (t, 7.4 Hz, 3H), 0.39 (dt, J =11.4, 7.4 Hz, 6H), -2.10 (s, 1H), -2.22 (s, 1H). UV-vis (CH₂Cl₂) λ_{max} (log ε): 392 (4.84), 414 (4.91), 497 (3.83), 532 (3.10), 632 (3.59), 660 (3.70), 693 (4.65). HR-MS (ESI+, 100% CH₃CN, TOF): m/z calc'd for C₃₆H₄₈N₄O₂, 568.3777 (for M⁺); found, 568.3747.

7,17-Dihydroxybacteriochlorin (7). Prepared in 48% yield (24 mg, 4.2×10^{-5} mol) from octaethyl-7,17-dioxobacteriochlorin **2** (50 mg, 8.82×10^{-5} mol) and LiAlH₄ (17 mg, 4.4×10^{-5} mol, 5 equiv) as described for the preparation of 7-hydroxychlorin **5**. MW = 570.8 g/mol; $R_f = 0.29$ (silica-CH₂Cl₂). ¹H NMR (400 MHz; DMSO- d_6): 9.00 (s, 2H), 8.62 (s, 2H), 6.41 (d, J = 5.7 Hz, 2H), 6.27 (d, J = 5.5 Hz, 2H), 3.87–3.76 (m, 8H), 2.44–2.38 (m, 6H), 2.09 (dt, J = 16.5, 6.3 Hz, 2H), 1.73–1.65 (m, 12H), 0.90 (t, J = 6.1 Hz, 6H), 0.54 (t, J = 6.0 Hz, 6H), -2.54 (s, 2H). UV-vis (CH₂Cl₂) λ_{max} (log ε): 350 (4.72), 375 (4.79), 464 (3.56), 496 (3.96), 713 (4.42). HR-MS (ESI +, 100% CH₃CN, TOF): m/z calc'd for $C_{36}H_{50}N_4O_2$, 570.3934 (for M⁺); found, 570.3893.

Crystallography. Crystals were grown of **2Ni**, **2Cu**, **2Pd**, and **2Ag** by slow vapor diffusion of hexanes into a concentrated solution of the species dissolved in CH_2Cl_2 . Single crystal data for **2Pd** were collected on a Bruker Quest diffractometer with a fixed χ -angle, a sealed tube fine focus X-ray tube, single crystal curved graphite incident beam monochromator, a Photon100 CMOS area detector and an Oxford Cryosystems low temperature device. Examination and data collection were performed with Mo K α radiation (λ = 0.71073 Å) at 150 K. Single crystal data for **2Ag**, **2Ni**, and **2Cu** were collected on a Bruker Quest diffractometer with κ -geometry, an I- μ -S microsource X-ray tube, laterally graded multilayer (Goebel) mirror single crystal for monochromatization, a Photon2 CMOS area detector and an Oxford

Cryosystems low-temperature device. Examination and data collection were performed with Cu K α radiation (λ = 1.54178 Å) at 150 K. Data were collected, reflections were indexed and processed, and the files were scaled and corrected for absorption using APEX3 and SADABS or TWINABS. The space groups were assigned and the structures were solved by direct methods using XPREP within the SHELXTL suite of programs and refined by full matrix least-squares against F^2 with all reflections using Shelxl2016 using the graphical interface ShelXle; for details, including on the software, see Supporting Information.

All four structures are isomorphic with close to identical molecular conformations, unit cell shapes, and symmetry and packing interactions. The structures are pseudo-B centered with a pseudo-translation along the a-c diagonal. Exact translational symmetry is broken by a slight modulation of the two gem-C(Et)₂ units, preventing an exact fit of a larger volume C-centered monoclinic structure. The b and c axes in the four structures are close in length, and the order of the two axes is swapped between the structures, thus resulting in different standard settings for the four isomorphic structures. Each of the two structures have the same standard setting: 2Ag and 2Cu, and 2Pd and 2Ni. The latter two were also found to be twinned by identical twin operations based on the emulated monoclinic symmetry (see Supporting Information for details on twinning).

If not specified otherwise, H atoms attached to carbon atoms were positioned geometrically and constrained to ride on their parent atoms with carbon hydrogen bond distances of 0.95 Å for aromatic C—H, and 0.99 and 0.98 Å for aliphatic CH₂ and CH₃ moieties, respectively. Methyl H atoms were allowed to rotate but not to tip to best fit the experimental electron density. $U_{\rm iso}({\rm H})$ values were set to a multiple of $U_{\rm eq}({\rm C})$ with 1.5 for CH₃, and 1.2 for CH₂ units, respectively.

Complete crystallographic data in CIF format have been deposited with the Cambridge Crystallographic Data Centre. CCDC 1955054—1955057 contain the supplementary crystallographic data for this paper. These data can be obtained free of charge from The Cambridge Crystallographic Data Centre via www.ccdc.cam.ac.uk/data request/cif.

Kinetic Comparison. A series of parallel reactions were conducted for porphyrin 4, oxochlorin 3, and dioxobacteriochlorin 2 to compare their relative metal-insertion reaction rates: 8.86×10^{-6} mol of 2 (5.0 mg), 3 (4.9 mg), and 4 (4.7 mg), as well as 5.0 equiv. $\text{Zn}(\text{OAc})_2.2\text{H}_2\text{O}$ (4.41 \times 10⁻⁵ mol, 9.7 mg) and Li_2CO_3 (15.0 mg) were combined in 25 mL three-necked round-bottom flasks equipped with a reflux condenser and stir bar. These three flasks were then all secured in the same oil bath. DMF (10 mL) was added simultaneously to all and the mixtures were set stirring and heated to reflux. Once refluxing, aliquots of ~10 μ L were periodically withdrawn and added to a small vial preloaded with 1.0 mL of HPLC-grade CH₂Cl₂. The frequency of withdrawal was chosen such that 10 samples were interspersed throughout the total reaction time. The vials were then capped, inverted to mix, and placed on dry ice until all of the samples were collected.

Once the reaction was complete, the samples were diluted to 3.0 mL with CH_2Cl_2 and a UV–vis spectrum of this solution was recorded. Then, each solution was spiked three times successively with a small (4–10 $\mu L)$ recorded volume of conc. solutions ($\sim\!0.8$ mM) of pure starting material, collecting a full UV–vis spectrum between each. Using the same solution, the same procedure was carried out using a concentrated solution of pure product, for a total of seven collected spectra per sample.

Data analysis consisted of constructing two successive-standard-addition plots, one for the starting material and one for the product. Single wavelengths were selected, one corresponding to either species. The generated plots were checked to ensure a linear response (r^2 value of greater than 0.998). In this plot, the x-intercept is taken to be the absolute value of the concentration of the analyte in the original solution. In this manner, the concentration of both materials was determined in the sample. This value was tracked back through the dilution procedure in order to determine the concentration of each in the reaction mixture at the time of withdrawal.

UV-visible Titrations. These were performed using a Varian Cary 100 spectrometer with a thermostated cell holder (held at 25 °C) in standard 1 cm (3 mL) cuvettes. Additions of the TFA stock solutions were pipetted to the concentrations indicated.

ASSOCIATED CONTENT

Supporting Information

The Supporting Information is available free of charge at https://pubs.acs.org/doi/10.1021/acs.inorgchem.9b03231.

A reproduction of the spectroscopic data and details to the titrations and crystallographic measurements (PDF)

Accession Codes

CCDC 1955054–1955057 contain the supplementary crystallographic data for this paper. These data can be obtained free of charge via www.ccdc.cam.ac.uk/data_request/cif, or by emailing data_request@ccdc.cam.ac.uk, or by contacting The Cambridge Crystallographic Data Centre, 12 Union Road, Cambridge CB2 1EZ, UK; fax: +44 1223 336033.

AUTHOR INFORMATION

Corresponding Author

Christian Brückner — Department of Chemistry, University of Connecticut, Storrs, Connecticut 06269-3060, United States; orcid.org/0000-0002-1560-7345; Email: c.bruckner@uconn.edu

Authors

David Schnable — Department of Chemistry, University of Connecticut, Storrs, Connecticut 06269-3060, United States; orcid.org/0000-0002-8650-997X

Nivedita Chaudhri — Department of Chemistry, University of Connecticut, Storrs, Connecticut 06269-3060, United States; orcid.org/0000-0001-9604-606X

Ruoshi Li – Department of Chemistry, University of Connecticut, Storrs, Connecticut 06269-3060, United States

Matthias Zeller — Department of Chemistry, Purdue University, West Lafayette, Indiana 47907-2084, United States;
orcid.org/0000-0002-3305-852X

Complete contact information is available at: https://pubs.acs.org/10.1021/acs.inorgchem.9b03231

Author Contributions

§D.S. and N.C. contributed equally.

Author Contributions

The manuscript was written through contributions of all authors. All authors have given approval to the final version of the manuscript. M.Z. performed the X-ray diffraction analyses.

Funding

Funding for this work was provided by the U.S. National Science Foundation (NSF) through Grants CHE-1465133 and CHE-1800631 (to C.B.) and CHE-1359081 (summer research fellowship to D.S.) and CHE-1625543 (X-ray diffractometers).

Notes

The authors declare no competing financial interest.

ACKNOWLEDGMENTS

We thank David Dolphin, University of British Columbia, and Chi-Kwong (Chris) Chang, Michigan State University, for donation of the octaethylporphyrin used in this study.

REFERENCES

- (1) Prinsep, M. R.; Caplan, F. R.; Moore, R. E.; Patterson, G. M. L.; Smith, C. D. Tolyporphin, a novel multidrug resistance reversing agent from the blue-green alga *Tolypothrix nodosa*. *J. Am. Chem. Soc.* 1992, 114 (1), 385–387.
- (2) Prinsep, M. R.; Patterson, G. M. L.; Larsen, L. K.; Smith, C. D. Further tolyporphins from the blue-green alga *Tolypothrix nodosa*. *Tetrahedron* **1995**, *51* (38), 10523–10530.
- (3) Prinsep, M. R.; Patterson, G. M. L.; Larsen, L. K.; Smith, C. D. Tolyporphins J and K, two further porphinoid metabolites from the cyanobacterium *Tolypothrix nodosa*. J. Nat. Prod. 1998, 61 (9), 1133–1136.
- (4) Barnhart-Dailey, M.; Zhang, Y.; Zhang, R.; Anthony, S. M.; Aaron, J. S.; Miller, E. S.; Lindsey, J. S.; Timlin, J. A. Cellular localization of tolyporphins, unusual tetrapyrroles, in a microbial photosynthetic community determined using hyperspectral confocal fluorescence microscopy. *Photosynth. Res.* **2019**, 141 (3), 259–271.
- (5) Minehan, T. G.; Cook-Blumberg, L.; Kishi, Y.; Prinsep, M. R.; Moore, R. E. Revised structure of tolyporphin A. *Angew. Chem., Int. Ed.* **1999**, 38 (7), 926–928.
- (6) Minehan, T. G.; Kishi, Y. Total synthesis of the proposed structure of (+)-tolyporphin A O, O-diacetate. Angew. Chem., Int. Ed. 1999, 38 (7), 923–925.
- (7) Wang, W.; Kishi, Y. Synthesis and structure of tolyporphin a *O*, *O*-diacetate. *Org. Lett.* **1999**, *1* (7), 1129–1132.
- (8) Liu, Y.; Zhang, S.; Lindsey, J. S. Total synthesis campaigns toward chlorophylls and related natural hydroporphyrins diverse macrocycles, unrealized opportunities. *Nat. Prod. Rep.* **2018**, 35 (9), 879–901.
- (9) Smith, C. D.; Prinsep, M. R.; Caplan, F. R.; Moore, R. E.; Patterson, G. M. L. Reversal of multiple drug resistance by tolyporphin, a novel cyanobacterial natural product. *Oncol. Res.* **1994**, *6* (4–5), 211–218.
- (10) Morliere, P.; Maziere, J.-C.; Santus, R.; Smith, C. D.; Prinsep, M. R.; Stobbe, C. C.; Fenning, M. C.; Golberg, J. L.; Chapman, J. D. Tolyporphin: A natural product from cyanobacteria with potent photosensitizing activity against tumor cells *in vitro* and *in vivo*. *Cancer Res.* **1998**, *58* (16), 3571–3578.
- (11) Prinsep, M. R.; Appleton, T. G.; Hanson, G. R.; Lane, I.; Smith, C. D.; Puddick, J.; Fairlie, D. P. Tolyporphin macrocycles from the cyanobacterium *Tolypothrix nodosa* selectively bind copper and silver and reverse multidrug resistance. *Inorg. Chem.* **2017**, *56* (10), 5577–5585
- (12) Buchler, J. W. Synthesis and properties of metalloporphyrins. In *The Porphyrins*; Dolphin, D., Ed.; Academic Press: New York, 1978; Vol. 1, pp 389–483.
- (13) Whitlock, H. W., Jr.; Hanauer, R.; Oester, M. Y.; Bower, B. K. Diimide reduction of porphyrins. J. Am. Chem. Soc. 1969, 91 (26), 7485–7489.
- (14) Brückner, C.; Samankumara, L.; Ogikubo, J. Syntheses of bacteriochlorins and isobacteriochlorins. In *Handbook of Porphyrin Science*; Kadish, K. M., Smith, K. M., Guilard, R., Eds.; World Scientific: River Edge, NY, 2012; Vol. 17, pp 1–112.
- (15) Krayer, M.; Yang, E.; Kim, H.-J.; Kee, H. L.; Deans, R. M.; Sluder, C. E.; Diers, J. R.; Kirmaier, C.; Bocian, D. F.; Holten, D.; Lindsey, J. S. Synthesis and photophysical characterization of stable indium bacteriochlorins. *Inorg. Chem.* **2011**, *50* (10), 4607–4618.
- (16) Chen, C.-Y.; Sun, E.; Fan, D.; Taniguchi, M.; McDowell, B. E.; Yang, E.; Diers, J. R.; Bocian, D. F.; Holten, D.; Lindsey, J. S. Synthesis and physicochemical properties of metallobacteriochlorins. *Inorg. Chem.* **2012**, *51* (17), 9443–9464.
- (17) Crossley, M. J.; Burn, P. L.; Langford, S. J.; Pyke, S. M.; Stark, A. G. A new method for the synthesis of porphryin-alpha-diones that is applicable to the synthesis of *trans*-annular extended porphyrin systems. J. Chem. Soc., Chem. Commun. 1991, 1567–1568.
- (18) Starnes, S. D.; Rudkevich, D. M.; Rebek, J., Jr. Cavitand-porphyrins. J. Am. Chem. Soc. 2001, 123 (20), 4659–4669.
- (19) Brückner, C.; Hyland, M. A.; Sternberg, E. D.; MacAlpine, J.; Rettig, S. J.; Patrick, B. O.; Dolphin, D. Preparation of [meso-

- tetraphenylchlorophinato]nickel(II) by stepwise deformylation of [meso-tetraphenyl-2,3-diformylsecochlorinato]nickel(II): Conformational consequences of breaking the structural integrity of nickel porphyrins. Inorg. Chim. Acta 2005, 358 (10), 2943–2953.
- (20) Hiroto, S.; Hisaki, I.; Shinokubo, H.; Osuka, A. Synthesis of directly and doubly linked dioxoisobacteriochlorin dimers. *J. Am. Chem. Soc.* **2008**, *130* (48), 16172–16173.
- (21) Lindsey, J. S. *De novo* synthesis of *gem*-dialkyl chlorophyll analogues for probing and emulating our green world. *Chem. Rev.* **2015**, *115* (13), 6534–6620.
- (22) Taniguchi, M.; Lindsey, J. S. Synthetic chlorins, possible surrogates for chlorophylls, prepared by derivatization of porphyrins. *Chem. Rev.* **2017**, *117* (2), 344–535.
- (23) Liu, M.; Chen, C.-Y.; Hood, D.; Taniguchi, M.; Diers, J. R.; Bocian, D. F.; Holten, D.; Lindsey, J. S. Synthesis, photophysics and electronic structure of oxobacteriochlorins. *New J. Chem.* **2017**, *41* (10), 3732–3744.
- (24) Connick, P. A.; Haller, K. J.; Macor, K. A. X-ray structural and imidazole-binding studies of nickel,-oxoporphyrins. *Inorg. Chem.* **1993**, 32 (15), 3256–3264.
- (25) Vairaprakash, P.; Yang, E.; Sahin, T.; Taniguchi, M.; Krayer, M.; Diers, J. R.; Wang, A.; Niedzwiedzki, D. M.; Kirmaier, C.; Lindsey, J. S.; Bocian, D. F.; Holten, D. Extending the short and long wavelength limits of bacteriochlorin near-infrared absorption via dioxo- and bisimide-functionalization. *J. Phys. Chem. B* **2015**, *119* (12), 4382–4395.
- (26) Hood, D.; Niedzwiedzki, D. M.; Zhang, R.; Zhang, Y.; Dai, J.; Miller, E. S.; Bocian, D. F.; Williams, P. G.; Lindsey, J. S.; Holten, D. Photophysical characterization of tolyporphin a, anaturally occurring dioxobacteriochlorin, and synthetic oxobacteriochlorin analogues. *Photochem. Photobiol.* **2017**, 93 (5), 1204–1215.
- (27) Guberman-Pfeffer, M. J.; Lalisse, R. F.; Hewage, N.; Brückner, C.; Gascón, J. A. Origins of the electronic modulations of bacterioand isobacteriodilactone regioisomers. *J. Phys. Chem. A* **2019**, *123* (34), 7470–7485.
- (28) Stolzenberg, A. M.; Glazer, P. A.; Foxman, B. M. Structure, reactivity, and electrochemistry of free-base β -oxoporphyrins and metallo- β -oxoporphyrin. *Inorg. Chem.* **1986**, 25 (7), 983–991.
- (29) Papkovsky, D. B.; Ponomarev, G. V.; Wolfbeis, O. S. Longwave luminescent porphyrin probes. *Spectrochim. Acta, Part A* **1996**, *52A* (12), 1629–1638.
- (30) Neal, T. J.; Kang, S.-J.; Turowska-Tyrk, I.; Schulz, C. E.; Scheidt, W. R. Magnetic interactions in the high-spin iron(III) oxooctaethylchlorinato derivative [Fe(oxoOEC)(Cl)] and its π-cation radical [Fe(oxoOEC•)(Cl)]SbCl₆. *Inorg. Chem.* **2000**, 39 (5), 872–880.
- (31) Neal, T. J.; Kang, S.-J.; Schulz, C. E.; Scheidt, W. R. Molecular structures and magnetochemistry of two (β-oxooctaethylchlorinato)-copper(II) derivatives: [Cu(oxoOEC)] and [Cu(oxoOEC•)]SbCl₆. *Inorg. Chem.* **1999**, 38 (19), 4294–4302.
- (32) Murphy, M. J.; Siegel, L. M.; Tove, S. R.; Kamin, H. Siroheme: A new prosthetic group participating in six-electron reduction reactions catalyzed by both sulfite and nitrite reductases. *Proc. Natl. Acad. Sci. U. S. A.* 1974, 71 (3), 612–616.
- (33) Chang, C. K. Synthesis and characterization of alkylated isobacteriochlorins, models of siroheme and sirohydrochlorin. *Biochemistry* **1980**, *19* (9), 1971–1976.
- (34) Chang, C. K.; Fajer, J. Models of siroheme and sirohydrochlorin. Π cation radicals of iron(II) isobacteriochlorin. *J. Am. Chem. Soc.* **1980**, *102* (2), 848–851.
- (35) Chang, C. K.; Barkigia, K. M.; Hanson, L. K.; Fajer, J. Models of heme d_1 . Structure and redox chemistry of dioxoisobacteriochlorins. *J. Am. Chem. Soc.* **1986**, *108* (6), 1352–1354.
- (36) Suh, M. P.; Swepston, P. N.; Ibers, J. A. Direct preparation of a siroheme model compound: Synthesis and structure of (5,10,15,20-tetramethylisobacteriochlorinato)nickel(II). *J. Am. Chem. Soc.* **1984**, *106* (18), 5164–5171.
- (37) Wei, Z.; Ryan, M. D. Infrared spectroelectrochemical reduction of iron porphyrin complexes. *Inorg. Chem.* **2010**, 49 (15), 6948–6954.

- (38) Tutunea, F.; Atifi, A.; Ryan, M. D. Visible and infrared spectroelectrochemistry of zinc and manganese porphinones: Metal vs. Porphyrin reduction. *J. Electroanal. Chem.* **2015**, *744*, 17–24.
- (39) Fujii, H.; Yamaki, D.; Ogura, T.; Hada, M. The functional role of the structure of the dioxoisobacteriochlorin in the catalytic site of cytochrome cd_1 for the reduction of nitrite. *Chem. Sci.* **2016**, 7 (4), 2896–2906.
- (40) Wu, Z.-Y.; Wang, T.; Meng, Y.-S.; Rao, Y.; Wang, B.-W.; Zheng, J.; Gao, S.; Zhang, J.-L. Enhancing the reactivity of nickel(II) in hydrogen evolution reactions (HERs) by β -hydrogenation of porphyrinoid ligands. *Chem. Sci.* **2017**, 8 (9), 5953–5961.
- (41) Ning, Y.; Jin, G.-Q.; Zhang, J.-L. Porpholactone chemistry: An emerging approach to bioinspired photosensitizers with tunable near-infrared photophysical properties. *Acc. Chem. Res.* **2019**, *52* (9), 2620–2633.
- (42) Andrews, L. E.; Bonnett, R.; Ridge, R. J.; Appelman, E. H. The preparation and reactions of porphyrin *N*-oxides. *J. Chem. Soc., Perkin Trans. 1* **1983**, 103–107.
- (43) Yu, C.; Kang, S.-J. Synthesis and characterization of $Cu(hfa)_2(\mu$ -1,4-dicyanobenzene) and Cu(2,13-dioxoOEIBC). *J. Korean Chem. Soc.* **2004**, 48 (4), 367–371.
- (44) Papkovsky, D. B.; Ponomarev, G. V. Spectral-luminescent study of the porphyrin-diketones and their complexes. *Spectrochim. Acta, Part A* **2001**, *57* (9), 1897–1905.
- (45) Zhang, S.; Nagarjuna Reddy, M.; Mass, O.; Kim, H.-J.; Hu, G.; Lindsey, J. S. Synthesis of tailored hydrodipyrrins and their examination in directed routes to bacteriochlorins and tetradehydrocorrins. *New J. Chem.* **2017**, *41* (19), 11170–11189.
- (46) Inhoffen, H. H.; Nolte, W. Zur weiteren Kenntnis des Chlorophyll und des Hämins. XXIV. Oxidative Umlagerungen am Octaäthylporphyrin zu Geminiporphin-polyketonen. *Justus Liebigs Ann. Chem.* **1969**, 725 (1), 167–176.
- (47) Fischer, H.; Gebhardt, H.; Rothhaas, A. Über Mesochlorin und Oxymesoporphyrine. *Liebigs Ann. Chem.* **1930**, 482 (1), 1–24.
- (48) Bonnett, R.; Dolphin, D.; Johnson, A. W.; Oldfield, D.; Stephenson, G. F. Oxidation of porphyrins with H₂O₂ in H₂SO₄. *Proc. Chem. Soc.* **1964**, 371–372.
- (49) Chang, C. K.; Sotiriou, C. Migratory aptitudes in pinacol rearrangement of *vic*-dihydroxychlorins. *J. Heterocycl. Chem.* **1985**, 22 (6), 1739–1741.
- (50) Chang, C. K.; Sotitiou, C.; Wu, W. Differentiation of bacteriochlorin and isobacteriochlorin formation by metallation. High yield synthesis of porphyrindiones via OsO₄ oxidation. *J. Chem. Soc., Chem. Commun.* 1986, No. 15, 1213–1215.
- (51) Adams, K. R.; Berenbaum, M. C.; Bonnett, R.; Nizhnik, A. N.; Salgado, A.; Valles, M. A. Second generation tumour photosensitisers: The synthesis and biological activity of octaalkyl chlorins and bacteriochlorins with graded amphiphilic character. *J. Chem. Soc., Perkin Trans. 1* **1992**, No. 12, 1465–1470.
- (52) Pandey, R. K.; Isaac, M.; MacDonald, I.; Medforth, C. J.; Senge, M. O.; Dougherty, T. J.; Smith, K. M. Pinacol-pinacolone rearrangements in *vic*-dihydroxychlorins and bacteriochlorins: Effect of substituents at the peripheral positions. *J. Org. Chem.* **1997**, *62* (5), 1463–1472.
- (53) Bonnett, R.; Nizhnik, A. N.; Berenbaum, M. C. Second generation tumor photosensitizers: The synthesis of octaalkylchlorins and bacteriochlorins with graded amphiphilic character. *J. Chem. Soc., Chem. Commun.* 1989, No. 23, 1822–1823.
- (54) Bonnett, R.; Nizhnik, A. N.; White, S. G.; Berenbaum, M. C. Porphyrin sensitizers in tumour phototherapy. Novel sensitizers of the chlorin and bacteriochlorin class with amphiphilic properties. *J. Photochem. Photobiol., B* **1990**, *6* (1–2), 29–37.
- (55) Morgan, A. R.; Garbo, G. M.; Keck, R. W.; Skalkos, D.; Selman, S. H. Synthesis and *in vivo* activity of some porphyrindione derivatives with potential in photodynamic therapy. *J. Photochem. Photobiol., B* **1990**, *6* (1–2), 133–141.
- (56) Hu, S.; Mukherjee, A.; Spiro, T. G. Synthesis, vibrational spectra, and normal mode analysis of nickel(II) 1,5-dihydroxy-1,5-

- dimethyloctaethylbacteriochlorin: A model for bacteriochlorophylls. J. Am. Chem. Soc. 1993, 115 (26), 12366–12377.
- (57) Ryppa, C.; Niedzwiedzki, D.; Morozowich, N. L.; Srikanth, R.; Zeller, M.; Frank, H. A.; Brückner, C. Stepwise conversion of two pyrrole moieties of octaethylporphyrin to pyridin-3-ones: Synthesis, mass spectral, and photophysical properties of mono and bis-(oxypyri)porphyrins. *Chem. Eur. J.* 2009, 15 (23), 5749–5762.
- (58) Ralphs, K.; Zhang, C.; James, S. L. Solventless mechanochemical metallation of porphyrins. *Green Chem.* **2017**, *19* (1), 102–105.
- (59) Atoyebi, A. O.; Brückner, C. Observations on the mechanochemical insertion of zinc(II), copper(II), magnesium(II), and select other metal(II) ions into porphyrins. *Inorg. Chem.* **2019**, *58* (15), 9631–9642.
- (60) Longo, F. R.; Brown, E. M.; Rau, W. G.; Adler, A. D. Kinetic and mechanistic studies of metalloporphyrin formation. In *The Porphyrins*; Dolphin, D., Ed.; Academic Press: New York, 1978; Vol. 5, pp 459–481.
- (61) Haddad, R.; Lu, Y.; Quirke, J. M. E.; Berget, P.; Sun, L.; Fettinger, J. C.; Leung, K.; Qiu, Y.; Schore, N. E.; van Swol, F.; Medforth, C. F.; Shelnutt, J. A. Steric bulkiness of pyrrole substituents and the out-of-plane deformations of porphyrins: Nickel(II) octaisopropylporphyrin and its meso-nitro derivative. J. Porphyrins Phthalocyanines 2011, 15 (07–08), 727–741.
- (62) Meyer, E. F., Jr. The crystal and molecular structure of nickel(II)octaethylporphyrin. *Acta Crystallogr., Sect. B: Struct. Crystallogr. Cryst. Chem.* **1972**, B28, 2162–2167.
- (63) Brennan, T. D.; Scheidt, W. R.; Shelnutt, J. A. New crystalline phase of (octaethylporphinato)nickel(II): Effects of π - π interactions on molecular structure and resonance Raman spectra. *J. Am. Chem. Soc.* **1988**, *110* (12), 3919–3924.
- (64) Buchler, J. W.; Buchler, J. W.; Eikelmann, G.; Puppe, L.; Rohbock, K.; Schneehage, H. H.; Weck, D. Metallkomplexe mit Tetrapyrrol-liganden, III. Darstellung von Metallkomplexen des Octaäthylporphins aus Metall-acetylacetonaten. *Justus Liebigs Ann. Chem.* 1971, 745 (1), 135–151.
- (65) Arkhypchuk, A. I.; Orthaber, A.; Kovacs, D.; Borbas, K. E. Isolation and characterization of a monoprotonated hydroporphyrin. *Eur. J. Org. Chem.* **2018**, 2018 (48), 7051–7056.
- (66) Stone, A.; Fleischer, E. B. The molecular and crystal structure of porphyrin diacids. J. Am. Chem. Soc. 1968, 90 (11), 2735–2748.
- (67) Oettmeier, W.; Janson, T. R.; Thurnauer, M. C.; Shipman, L. L.; Katz, J. J. Spectroscopic characterization of the pheophytin a dication. *J. Phys. Chem.* **1977**, *81* (4), 339–342.
- (68) Walter, R. I.; Ojadi, E. C. A.; Linschitz, H. A proton NMR study of the reactions with acid of *meso*-tetraphenylporphyrins with various numbers of 4-(dimethylamino) groups. *J. Phys. Chem.* **1993**, 97 (50), 13308–13312.
- (69) Cavaleiro, J. A. S.; Jackson, A. H.; Ali, S. A. The protonation of chlorins (dihydroporphyrins). *Tetrahedron Lett.* **1984**, 25 (2), 229–232.
- (70) Ke, X.-S.; Chang, Y.; Chen, J.-Z.; Tian, J.; Mack, J.; Cheng, X.; Shen, Z.; Zhang, J.-L. Porphodilactones as synthetic chlorophylls: Relative orientation of β -substituents on a pyrrolic ring tunes NIR absorption. *J. Am. Chem. Soc.* **2014**, *136* (27), 9598–9607.
- (71) Ke, X. S.; Zhao, H.; Zou, X.; Ning, Y.; Cheng, X.; Su, H.; Zhang, J. L. Fine-tuning of β-substitution to modulate the lowest triplet excited states: A bioinspired approach to design phosphorescent metalloporphyrinoids. *J. Am. Chem. Soc.* **2015**, *137* (33), 10745–10752.
- (72) Hewage, N.; Daddario, P.; Lau, K. S. F.; Guberman-Pfeffer, M. J.; Gascón, J. A.; Zeller, M.; Lee, C. O.; Khalil, G. E.; Gouterman, M.; Brückner, C. Bacterio- and isobacteriodilactones by stepwise or direct oxidations of *meso*-tetrakis(pentafluorophenyl)porphyrin. *J. Org. Chem.* **2019**, *84* (1), 239–256.
- (73) Mahammed, A.; Weaver, J. J.; Gray, H. B.; Abdelas, M.; Gross, Z. How acidic are corroles and why? *Tetrahedron Lett.* **2003**, 44 (10), 2077–2079.
- (74) Khalil, G. E.; Daddario, P.; Lau, K. S. F.; Imtiaz, S.; King, M.; Gouterman, M.; Sidelev, A.; Puran, N.; Ghandehari, M.; Brückner, C.

- meso-Tetraarylporpholactones as high pH sensors. Analyst 2010, 135 (8), 2125-2131.
- (75) Worlinsky, J. L.; Halepas, S.; Brückner, C. PEGylated meso-arylporpholactone metal complexes as optical cyanide sensors in water. *Org. Biomol. Chem.* **2014**, *12* (23), 3991–4001.
- (76) Worlinsky, J. L.; Halepas, S.; Ghandehari, M.; Khalil, G.; Brückner, C. High pH sensing with water-soluble porpholactone derivatives and their incorporation into a Nafion® optode membrane. *Analyst* **2015**, *140* (1), 190–196.
- (77) Liu, E.; Ghandehari, M.; Brückner, C.; Khalil, G.; Worlinsky, J.; Jin, W.; Sidelev, A.; Hyland, M. A. Mapping high pH levels in hydrated calcium silicates. *Cem. Concr. Res.* **2017**, *95*, 232–239.
- (78) Stolzenberg, A. M.; Steshic, M. T. Reductive chemistry of nickel hydroporphyrins. Evidence for a biologically significant difference porphyrins, hydroporphyrins, and other tetrapyrroles. *J. Am. Chem. Soc.* **1988**, *110* (19), 6391–6402.
- (79) Papkovsky, D. B.; Ponomarev, G. V.; Trettnak, W.; O'Leary, P. Phosphorescent complexes of porphyrin ketones: Optical properties and application to oxygen sensing. *Anal. Chem.* **1995**, *67* (22), 4112–4117.